ROYAL SOCIETY
OF CHEMISTRY

PAPER

Check for updates

A "turn-on" fluorescence resonance energy transfer aptasensor based on carbon dots and gold nanoparticles for 17β-estradiol detection in sea salt†

Tianrun Qian,‡[ab] Jia Bao,‡[c] Xuepeng Liu,[a] Gerile Oudeng[d] and Weiwei Ye [ID] *[ae]

17β-estradiol is abused in the food industry. Excess 17β-estradiol can disturb the endocrine system or cause many diseases including obesity, diabetes, cardiac-cerebral vascular disease, and cancers in the human body. A "turn-on" fluorescence resonance energy transfer (FRET) aptasensor based on carbon dots (CDs) and gold nanoparticles (AuNPs) was developed for the detection of 17β-estradiol. A thiol-modified oligonucleotide was conjugated to AuNPs and amino modified oligonucleotide was linked to CDs. The 17β-estradiol aptamer was hybridized with the two oligonucleotides, shortening the distance between CDs and AuNPs. With 360 nm UV light excitation, FRET occurred between CDs and AuNPs. The system was "turn-off". When 17β-estradiol was detected, the aptamer specifically bound to 17β-estradiol, and the FRET system was destroyed, leading to the "turn-on" phenomenon. The fluorescence intensity recovery was detected in the concentration range of 400 pM to 5.5 μM. The limit of detection (LOD) was 245 pM. The FRET aptasensor demonstrated good selectivity for 17β-estradiol detection. Reasonable spiked recoveries were obtained in sea salt samples. It showed the potential for estrogen detection in food safety and environmental applications.

1. Introduction

Endocrine disrupting chemicals (EDCs) exist widely in food, soil, air and water.[1,2] 17β-estradiol is a typical EDC and one of the most potent estrogenic compounds among natural steroid estrogens.[3] It can interfere with the normal endocrinal functions of the human body and animals, thereby affecting the intracellular signaling processes and physiological functions, such as growth, development and reproduction. 17β-estradiol is widely used in animal feed to promote animal growth, leading to a high level of estrogen in dairy and meat. The addition of estrogen is strictly forbidden in the food industry by the European Union.[4] Besides, 17β-estradiol is abused in contraception

and clinical treatments.[5] After ingesting food with 17β-estradiol residue or taking drugs with large amounts of 17β-estradiol, these compounds will enter the human body and are often eliminated very slowly. Excess 17β-estradiol and its metabolites may disturb the endocrine system, causing sexual abnormalities, obesity, diabetes, cardiac–cerebral vascular disease, a decline in male birth rates, and even induce cancer.[6,7] Therefore, it is very important to detect 17β-estradiol to avoid excess intake.

Classic methods, including high performance liquid chromatography (HPLC) and chromatography tandem mass spectrometry have accuracy and sensitivity for detecting 17β-estradiol. Most of them require expensive instruments, complicated and expensive sample preparation, large amounts of harmful organic solvents and tedious procedures.[8–10] Enzyme-linked immunosorbent assay (ELISA) can be used to detect 17β-estradiol specifically and sensitively.[11] ELISA depends on the interaction between antigen and antibody, which varies with different batches. It is prone to false positive results. The electrochemical analysis methods have high sensitivity and fast analysis speed, but the stability and reproducibility are affected by electrode properties.[12] Fluorescence resonance energy transfer (FRET) process occurs between a pair of light-sensitive molecules, where the fluorescence donor, initially in its electronic excited state, transfers energy to an acceptor within a close proximity.[13] FRET biosensors consist of

[a] College of Mechanical Engineering, Zhejiang University of Technology, Hangzhou 310014, People's Republic of China. E-mail: yeweiwei@zjut.edu.cn

[b] College of Food Science and Technology, Zhejiang University of Technology, Hangzhou 310014, People's Republic of China

[c] The Science Technology Department of Zhejiang Province, Hangzhou 310006, People's Republic of China

[d] Department of Hematology and Oncology, Shenzhen Children's Hospital, Shenzhen 518000, People's Republic of China

[e] Ninghai ZJUT Academy of Science and Technology, Ningbo 315615, People's Republic of China

‡ Tianrun Qian and Jia Bao contributed equally to this work.

a pair of fluorescence donor and acceptor and realize target detection based on the FRET principle. They have been widely used for monitoring environmental changes and examining the interaction between molecules.[14–17] FRET biosensors are prevalent among optical biosensors and have become valuable tools in 17β-estradiol analysis due to their sensitivity and simplicity.[18]

The recognition elements of FRET biosensors are the core part because they act as the key role in capturing targets of interest. Antibodies are widely used recognition elements in FRET biosensor development.[19] However, the accuracy requirements of the antibodies to anchor in biosensors, as well as high cost and poor stability restrict the use of antibodies. Aptamers are artificially synthesized oligonucleotides, which can fold into secondary structures or unique complex three-dimensional structures. These structures bind to specific targets with high selectivity. Moreover, the binding process does not damage the original structure of aptamers.[20] Aptamers have attracted considerable attention in the fields of biological analysis, such as small molecule detection, targeted therapy, and clinical diagnosis.[21,22] The development of aptasensor has great application prospects due to their advantages including simple operation, no limitation for target detection, and ease of reproduction.

Quantum dots (QDs) are excellent fluorescent materials that have been widely used in the construction of FRET biosensors. Many fluorescence analysis methods use semiconductor QDs or organic dyes as fluorescent donors. A FRET aptasensor based on a fluorescence dye label as the donor and a spherical graphite nanoparticle as the fluorescent nanoquencher was developed for 17β-estradiol detection.[23] However, semiconductor QDs are highly toxic, and organic dyes are easy to photobleach and have poor light stability.[24] Carbon dots (CDs) have the advantages of low toxicity, low cost, and environmental friendliness. The surfaces of CDs are rich in functional groups, which can be easily modified by biomolecules including aptamers and antibodies.[25,26] CDs have been widely used in optical biosensing and environmental pollutant detection.[27] AuNPs have large surface area to volume ratio and wide absorption spectrum. The spectra of CD emission and AuNP absorption overlapped in the wavelength range of 400 to 600 nm. It makes CDs and AuNPs efficient fluorescence donors and quenchers of FRET aptasensors for estrogen detection.[28–30]

In the study, a novel FRET aptasensor based on CDs and AuNPs as the donor and acceptor pairs has been developed for 17β-estradiol detection. CDs were modified with oligonucleotides (F1) by linkage between carboxyl group and amino group. AuNPs was functionalized with oligonucleotides (F2) by strong Au–S bond. The hybridization of F1 and F2 with aptamers (Apt) forms the CDs-F1-Apt-F2-AuNP assembly, bringing CDs and AuNPs in a close proximity. When the CDs were excited by 360 nm UV light, the emission of CD energy transferred to AuNPs, and FRET effect occurred. The detection of target 17β-estradiol, which interacts with aptamer specifically, destroyed CDs-F1-Apt-F2-AuNPs assembly. CDs and AuNPs were separated and fluorescence was recovered. The target 17β-estradiol was detected by analyzing the fluorescence recovery rate. The limit of detection (LOD) of this FRET aptasensor for 17β-estradiol detection was 245 pM. It shows the potential for estrogen detection with high sensitivity and selectivity in food safety applications.

2. Materials and methods

2.1. Materials

Specifically, chloroauric acid (HAuCl$_4$), sodium citrate, phosphate buffered saline (PBS), 1-(3-dimethylaminopropyl)-3-ethylcarbodiimide (EDC), diethylenetriamine (DETA), citric acid, N-hydroxy succinimide (NHS) and tris–HCl were purchased from Sigma-Aldrich (St. Louis, Missouri (Mo), USA). Dithiothreitol (DTT), 17β-estradiol, hydrocortisone, estriol, estrone, NaCl, KCl and filter membrane (0.45 μm) were obtained from ALADDIN Reagent (Shanghai, China). Potassium carbonate and nitric acid (HNO$_3$, 98% w/w) were ordered from Shanghai Lingfeng Chemical Reagent Co., Ltd (Shanghai, China). Ethanol and hydrochloric acid (HCl, 37% w/w) were bought from Xilong Science Co., Ltd (Guangdong, Shantou, China). Gel columns (illustra MicrospinG-25 Columns) were purchased from GE healthcare (UK). The 17β-estradiol aptamer (5′-AAGGGATGCCGTTTGGGCCCAAGTTCGGCATAGTG-3′, Apt),[31] amino-modified oligos (5′-TCCCTTAAAAAA-3′-NH$_2$, F1) and thiol-modified oligos (SH-5′-AAAAAACACTAT-3′, F2) were provided by Sangon Biotech (Shanghai) Co., Ltd (Shanghai, China).

2.2. Preparation of carbon dots (CDs)

CDs were prepared via one-step hydrothermal synthesis from citric acid and DETA.[32] A Teflon-equipped stainless steel autoclave was cleaned and dried. Citric acid (0.22 g) was dissolved in deionized (DI) water (10 mL) and DETA (112.6 μL) was added under stirring. The mixture was transferred into the autoclave and reacted at 200 °C. Dark brown solution was obtained after 6 h. CDs were collected from the dark-brown solution by freeze-drying technology. They were dispersed in DI water for characterization and further use.

2.3. Surface modification of CDs

CD solution was firstly ultrasonicated for 10 min. EDC/NHS (30 μL, 13 mM/13 mM) solution was added to the CDs (0.5 μL, 3 mg mL^{-1}). The mixed solution was vortexed and then ultrasonicated for 20 min. The solution system was adjusted to about pH 5.0 by hydrogen chloride. Amino-modified oligo F1 (2.5 μL, 100 μM) was incubated with CDs for 24 h at 4 °C to form CDs-F1 conjugation. CDs-F1 conjugation was stored at 4 °C for later use.

2.4. Synthesis of gold nanoparticles (AuNPs)

AuNPs were synthesized from sodium citrate reduction of chloroauric acid. Three-neck flask, magnetic stir bar and condenser pipe were washed in aqua regia and rinsed thoroughly in DI water. HAuCl$_4$ (20 μL, 14.3 wt%) was added to boiled DI water (40 mL) with refluxing and vigorous stirring. Then, the solution of sodium citrate (7.2 mL, 1 wt%) was rapidly added with stirring. The solution was heated and stirred until it

turned wine red, indicating the formation of AuNPs. AuNPs solution was cooled under continuous stirring and refluxing. They were stored at 4 °C in a dark environment. The size and concentration of prepared AuNPs could be characterized by the UV absorbance spectrum and scanning electron microscopy, respectively.

2.5. Surface functionalization of AuNPs

The disulfur linkage of thiol modified oligo F2 (19.2 μL, 100 μM) should be cleaved by DTT (1 M, pH 8.2) for 40 min at 25 °C to improve the immobilization efficiency of F2 on AuNPs. The remaining DTT was removed through gel-columns under centrifugation at 4600 rpm for 2 min. The purified F2 was mixed with AuNP solution (500 μL) and reacted under stationary condition at room temperature for 24 h. Then, PBS (0.1 M) was slowly added to the mixture. While standing for 16 h, F2 was conjugated on AuNPs. The F2-AuNP conjugation was purified by centrifugation (14 000 rpm, 3 min). The supernatant was removed, and the remaining red sediment was rinsed with DI water thrice. The F2-AuNP conjugation was dispersed in PBS for later experiments.

2.6. Characterization

The size and morphology of CDs and AuNPs were characterized by a transmission electron microscopy (TEM, JEOL-2100F, Japan). Atomic force microscopy (AFM) images were obtained on Bruker ICON AFM (Bruker, MA, USA). Fourier transform infrared (FTIR) spectrum was obtained from Nicolet 6700 spectrometer (Thermo-Fisher, USA), which worked at room temperature with the ambient humidity of 45% RH. The UV absorbance spectra were determined using Synergy H1 hybrid multi-mode microplate reader (Biotek, Vermont, USA). Time-resolved fluorescence measurement was performed on FLS-1000 (Edinburgh Instruments, UK). Circular Dichroism (CD) spectra were measured using a Chirascan J-815 spectrometer (Jasco, Japan).

2.7. FRET aptasensor for 17β-estradiol detection

DNA hybrid buffer solution (pH 7.4), including tris–HCl (25 mM), NaCl (140 mM), and KCl (10 mM) was prepared. The functionalized CDs-F1 was mixed with 17β-estradiol aptamer (2.5 μL, 100 μM) and purified F2-AuNPs (69 μL) in the DNA hybrid buffer solution at room temperature for 1 h. Various concentrations of 17β-estradiol were added and incubated for 15 min. The fluorescence intensity change for 17β-estradiol detection was performed on F2700 (Hitachi, Japan). The selectivity of FRET aptasensor was studied under the interference of hydrocortisone, estriol, estrone, diethylstilbestrol and hexestrol at the same concentrations of 100 nM and 1 nM.

2.8. Real sample analysis

Sea salt samples (snowave) were purchased from a local supermarket (Vanguard Co. Ltd, Hangzhou, China). Sea salt (2.0 g) was weighed and dissolved in DI water (18 mL). The solution was filtrated with a filter membrane (0.45 μm), and collected in

Eppendorf tube (50 mL) for the detection of 17β-estradiol. Then a certain amount of 17β-estradiol was added into the sea salt sample for the recovery tests.

3. Results

3.1. Mechanism of FRET aptasensor

The principle of 17β-estradiol detection by FRET aptasensor based on CDs as fluorescence donors and AuNPs as quenchers was shown in Fig. 1.[30] CDs have the maximum emission at 443 nm wavelength under 360 nm UV excitation. Amino modified oligos (F1) was fixed on the surface of CDs *via* the coupling reaction of amino and carboxyl group on the surface of CDs with EDC/NHS as the linker. Thiol-modified oligos (F2) were conjugated on AuNPs by strong Au–S covalent binding. The 17β-estradiol aptamer was used to co-hybridize with F1 and F2, resulting in a CDs-F1-Apt-F2-AuNPs assembly, reducing the distance between CDs and AuNPs within 10 nm. With 360 nm UV light excitation, the fluorescence energy of CDs was transferred to AuNPs. FRET occurred and the fluorescence was "turn-off", which was characterized by the decrease of fluorescence intensity. When 17β-estradiol was detected, the aptamer was specifically bound to 17β-estradiol and the co-hybridized assembly was destroyed. Therefore, the CDs and AuNPs were separated in the solution and their distance became large. When CDs were excited by UV light, the fluorescence intensity recovered, leading to the "turn-on" of the system. By measuring the specific changes of fluorescence intensity, 17β-estradiol can be detected.

3.2. Characterization of AuNPs and CDs

TEM was applied to characterize the sizes and morphology of AuNPs and CDs. The AuNPs dispersed well in DI water with TEM results shown in Fig. 2a. AuNPs had a well-rounded shape with the average particle size of about 25 nm (Fig. 2b). Fig. 2b inset shows that AuNPs were wine red in color and stable in solution. As shown in Fig. 2c, a layer of single oligonucleotide existed around AuNPs, demonstrating the successful modification of F2 on AuNPs.[28] CDs were spherical and well-dispersed in DI water (Fig. 2d), and their diameter ranged from 2 to 5 nm. Fig. 2e and f show the typical AFM images of CDs, which showed that CDs were in the monodispersion state. The diameters of CDs obtained from AFM and TEM were consistent.[33] Assembly of CDs-F1-Apt-F2-AuNPs was characterized *via* TEM. Hybridization of aptamer with F1 and F2 made CDs appear close to AuNPs within 10 nm. AuNPs were surrounded by CDs (Fig. S1a†). When 17-estradiol was detected, the distance between CDs and AuNPs was large (Fig. S1b†). Under UV light excitation, CDs suspension exhibited blue photoluminescence (Fig. 2d inset). The fluorescence of CDs was dependent on the excitation wavelength. To confirm the best excitation wavelength of CDs, fluorescence spectrum was scanned with different excitation wavelengths. As shown in Fig. S2,† the best excitation wavelength of CDs was 360 nm, and the best emission wavelength was 443 nm.
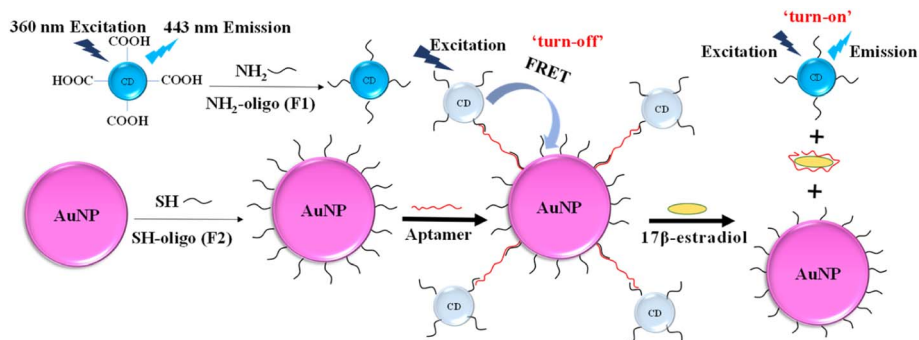
Fig. 1 Mechanism of "turn-on" FRET aptasensor for 17β-estradiol detection.

The coupling between CDs and F1 was characterized by FTIR. The characteristic absorption peak of CDs-F1 appeared at 1644.5 cm^{-1} and 1709 cm^{-1}, showing amide vibration. It confirmed that the amide bond between CDs and F1 was successfully formed *via* EDC/NHS method (Fig. S3†). In addition, the absorption peak at 1088 cm^{-1} was generally attributed to the C–O stretching of the DNA main chain.[34]

The measurement of circular dichroism spectra was implemented to characterize the conformation change of aptamer after the binding of 17β-estradiol. As illustrated in Fig. S4,† the
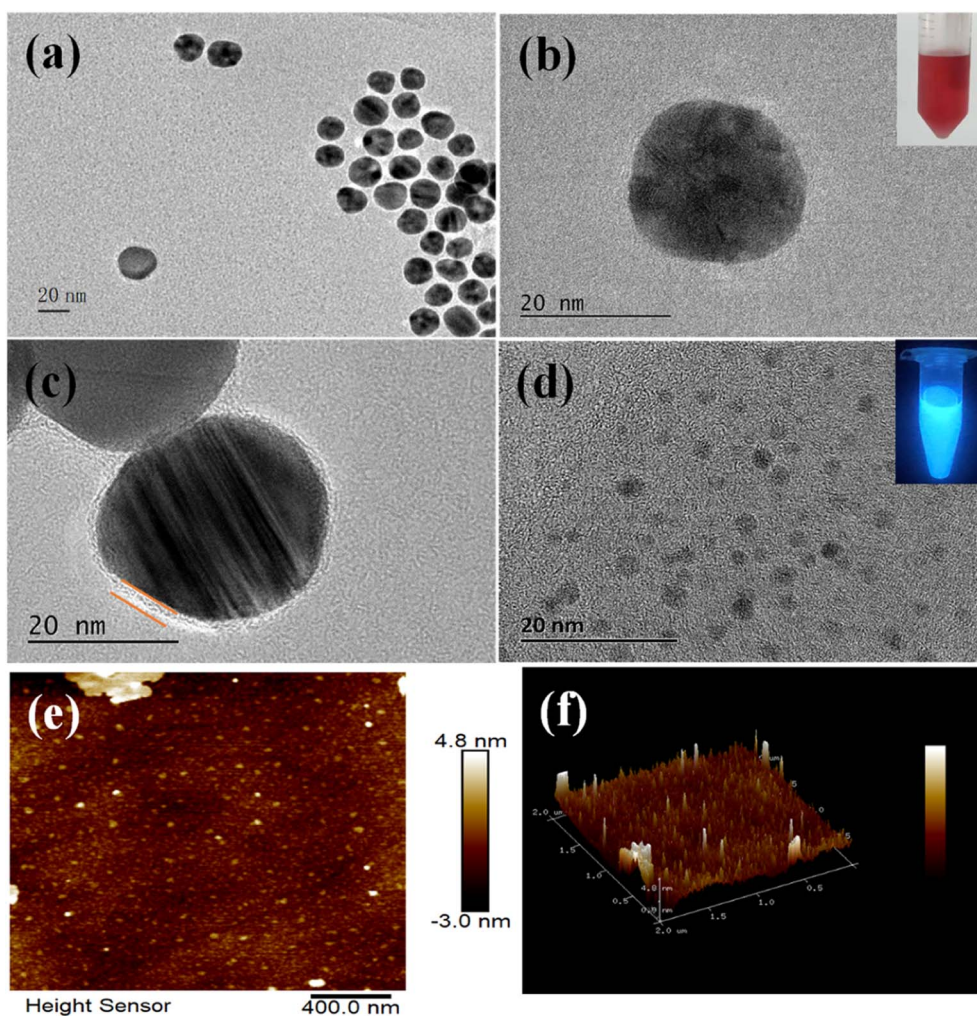

Fig. 2 (a) TEM images of AuNPs with good dispersion in solution; (b) TEM image with a single AuNP; (inset) wine red color of AuNP solution; (c) TEM image of F2-AuNPs conjugation; (d) TEM image of CDs with average size of 5 nm; (inset) color of CDs solution under UV excitation; (e) and (f) AFM images of CDs.

circular dichroism spectrum of aptamer exhibited a positive peak at 280 nm and a negative band at 248 nm. Nevertheless, in the presence of 17β-estradiol, owing to the specific binding of aptamers with 17β-estradiol, a decrease in the intensities of both positive and negative bands appear without a shift in the band position. The reduction of circular dichroism amplitude indicated the existence of hairpin structure of aptamers, which could be ascribed to the folding of random coil aptamers into the hairpin structure caused by the formation of aptamer–estradiol complex.[35]

3.3. Absorption property of AuNPs and emission of CDs

In the wavelength range of 300 to 700 nm, the AuNPs presented broad UV/Vis absorption. The maximum absorption peak was located at 522 nm. Additionally, the maximum absorption wavelength shifted from 522 nm of AuNPs to 525 nm wavelength of F2-AuNPs (Fig. 3a). The conjugation of F2 to AuNPs enlarged the nanoparticle size. Owing to the weak change of surface electromagnetic field caused by the replacement of citric acid molecules on the surface of AuNPs by F2, the absorption spectrum showed a red shift after connecting with F2. CDs can be excited with various wavelengths, and the photoluminescence emission change from violet to yellow.[36] Fig. 3b shows the intense fluorescence of CDs with the maximum emission at 443 nm. The spectra of CDs emission and AuNP absorption overlapped in the wavelength range of 400 to 600 nm. It made the energy transfer between CDs and AuNPs feasible in the FRET aptasensor. The phenomenon of FRET was confirmed by fluorescence lifetime measurements (Fig. S5†). The excitation and the emission wavelength of the pulse laser was 360 nm and 443 nm, respectively. The time-resolved fluorescence spectra of CDs, CDs-F1 and CDs-F1 after addition of 17β-estradiol showed no significant changes. The fluorescence lifetime of CDs was fitted and listed in Table S1.† It included a short lifetime component (τ_1) and a long lifetime component (τ_2). It was speculated that the two lifetime components of CDs may be attributed to the carbon center and surface traps, respectively.[37] The fluorescence lifetime of CDs was 5.79 ns, which decreased to 5.5 ns after conjugation with F1. The average fluorescence lifetime of CDs-F1 was 6.78 ns after the addition of 17β-estradiol. The lifetime of CDs, CDs-F1 and CDs-F1 after the addition of 17β-estradiol was similar. It confirmed that fluorescence intensity decreased between CDs and AuNPs was due to the FRET phenomenon.

3.4. Optimization of the experimental conditions

The photoluminescence of CDs was affected by the pH conditions. As shown in Fig. 4a, under 360 nm UV light excitation, the fluorescence spectra varied with different pH solutions. In acidic solution, the fluorescence intensity was relatively low,
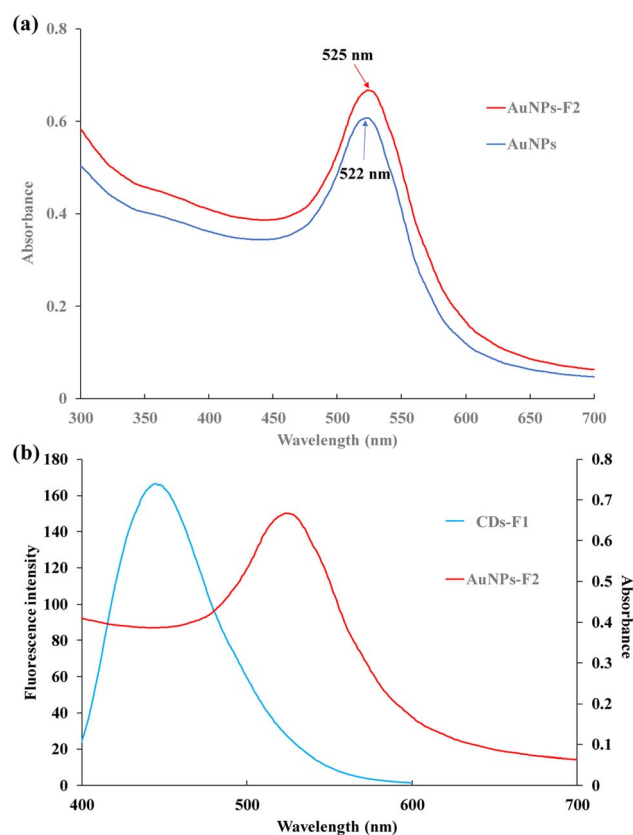

Fig. 3 (a) Absorption spectra of AuNPs and F2-AuNPs conjugation; (b) emission spectrum of CDs and absorption spectrum of AuNPs.
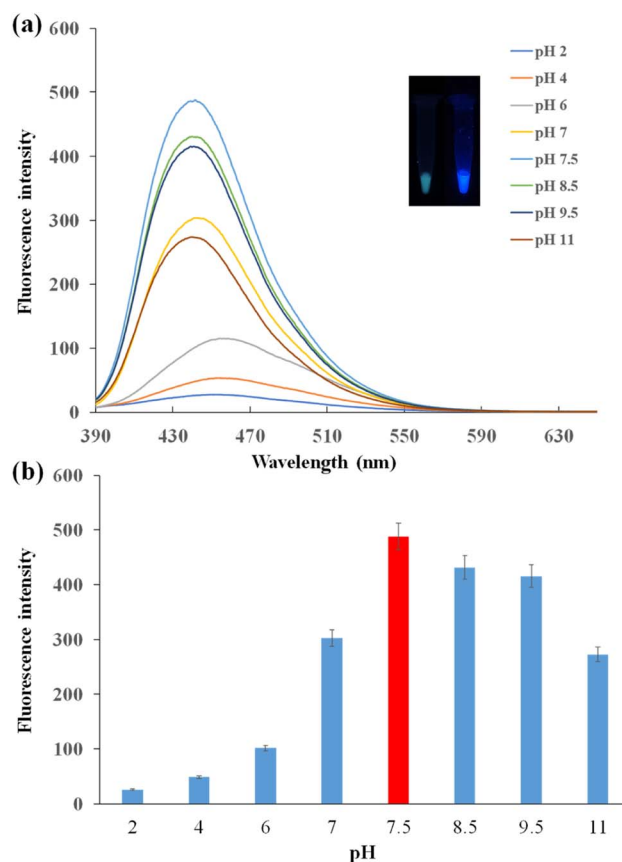

Fig. 4 (a) Fluorescence emission spectra of CDs under different pH; (inset) CDs presented green with pH 2 and presented blue with pH 11; (b) fluorescence intensity change under different pH conditions.
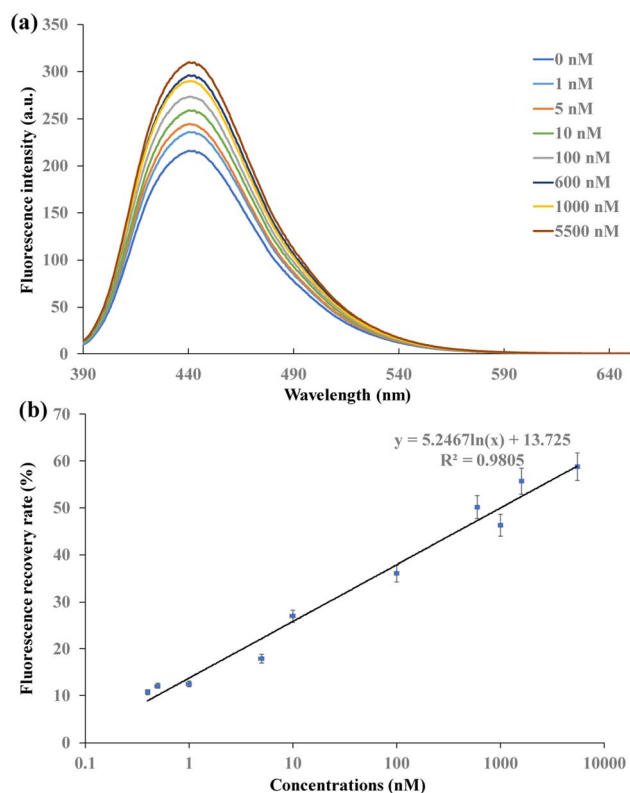
Fig. 5 (a) Fluorescence intensity under different concentrations of 17β-estradiol, (b) fluorescence intensity recovery efficiency at different concentrations of 17β-estradiol.

Fig. 6 Recovery efficiency comparison among estradiol, hydrocortisone, estriol, diethylstilbestrol and hexestrol with concentration of 100 nM.

and the peak of the spectrum had a bathochromic shift. The fluorescence intensity increased with the increasing pH. The fluorescence intensity was the lowest with pH 2 and the highest with pH 7.5. This was because the functional groups of CDs were protonated in acidic solution, and CDs were interacted with H^+ ions leading to the decrease in fluorescence intensity. In alkaline solution, fluorescence intensity decreased with the pH increase.[38] The urea groups were hydrolyzed gradually, diminishing the intramolecular H-bonding in urea groups. It may be the reason for the decrease of fluorescence intensity of CDs in the alkaline solution.[39] Under 360 nm UV light excitation, CDs turned green under pH 2 and presented blue under pH 11 (Fig. 4a inset). The fluorescence intensity change was
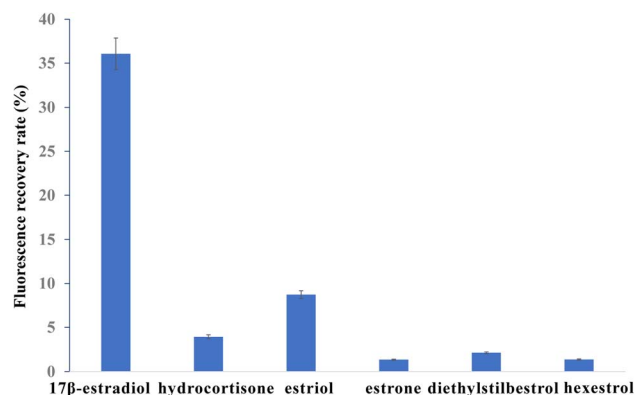
shown clearly in Fig. 4b. The best working condition of CDs was observed in the buffer of pH 7.5.

To optimize the AuNP concentrations in the FRET system, various concentrations of AuNPs were added to the CDs-F1 conjugation bound with the aptamer. The fluorescence of CDs was quenched by AuNPs. When the AuNPs had the concentration of 0.056 nM, the quenching efficiency reached the maximum (Fig. S6†). When the concentration of AuNPs was fixed, the aptamers were titrated to obtain the most suitable amount in the FRET system. The quenching efficiency increased with the increase in the aptamer concentrations from 0.1 μM to 2 μM. When the aptamer concentrations were larger than 2 μM, the quenching efficiency remained almost unchanged (Fig. S7†). The best concentration of aptamers was 2 μM.

3.5. Detection of 17β-estradiol by the FRET aptasensor

In the CDs and AuNPs based FRET aptasensor, the distance between the CDs and AuNPs became shorter when aptamer hybridized with oligonucleotides that were immobilized on their surfaces. With the excitation of CDs by 360 nm UV light, FRET occurred, and the signal was "turn-off". The specific reaction of the aptamer with 17β-estradiol separated CDs and AuNPs, leading to the signal "turn-on". To investigate the performance of this FRET aptasensor, different concentrations of 17β-estradiol ranging from 400 pM to 5.5 μM were detected. The fluorescence recovery efficiency of the FRET aptasensor and

Table 1 An overview on recently reported sensors for detection of 17β-estradiol

Method	Material	Analytical range	LOD	Ref.
Enzyme sensor	CA-GR/GCE	0.4–57 pM	0.13 pM	40
Electrochemical sensor	Wrinkled mesoporous carbon (wMC)	0.05–80.0 μM	8.3 nM	41
Fluorescence	Ru complex/QDs	0.08–0.4 μM	37 nM	42
Electrochemical sensor	CPE-CeO₂	10–100 nM	1.3 nM	43
Electrochemical sensor	CDs-PANI/GCE	0.001–100 μM	43 nM	44
Phosphorescence aptasensor	PLNPs-Apt/MoS₂	0.5–1.2 μg mL⁻¹	0.29 ng mL⁻¹	45
Voltammperometric biosensor	RhCl₃/graphene oxide with NaBH₄	0.9–11 pM	0.54 pM	46
Electrochemical sensor	CuPc-P6LC-Nafion/SPEF	0.08–7.3 μM	5.0 nM	47
Fluorescence	CDs/AuNPs	400 pM to 10 μM	245 pM	This work

Table 2 The application of FRET aptasensor for analysis of sea salt samples spiked with different amounts of 17β-estradiol

Sample	Analytes	Found value (nM)	Spiked level (nM)			
Sea salt (snowave)	17β-estradiol	N.D.[b]	0.4	5	50	500
			Ac.[c] (nM)	Ac. (nM)	Ac. (nM)	Ac. (nM)
			0.3202	5.631	57.18	442.13
			Re.[a] (%)	Re. (%)	Re. (%)	Re. (%)
			80.1	112.6	114.2	88.4

[a] Re.: recovery. [b] N.D.: not detected. [c] Ac.: actual measured values.

the concentrations of 17β-estradiol were explored. Based on the relationship of fluorescence recovery efficiency and 17β-estradiol concentrations, the LOD of this FRET aptasensor can be obtained.

The fluorescence spectra of CDs-F1 with the addition of F2-AuNPs and various concentrations of 17β-estradiol are shown in Fig. S8† and 5a, respectively. The fluorescence intensity increased with the increase in the 17β-estradiol concentrations under 360 nm excitation. When the high concentration of 17β-estradiol was detected, a large amount of aptamers were interacted with 17β-estradiol. Due to the destruction of CDs-F1-Apt-F2-AuNP structure after the addition of 17β-estradiol, CDs and AuNPs were separated, leading to fluorescence recovery. As shown in Fig. 5b, fluorescence recovery efficiency increased gradually with the increase in 17β-estradiol concentration. The recovery efficiency can be expressed by $R_e = (F_q - F_0)/(F_r - F_0) \times 100\%$, where F_r is the fluorescence intensity of CDs-F1 with addition of F2-AuNPs only, F_q is the fluorescence intensity of 17β-estradiol detection, and F_0 is the fluorescence intensity without 17β-estradiol addition. The linear relationship of fluorescence recovery efficiency and 17β-estradiol concentrations can be expressed as $R_e = 5.2457 \ln(C) + 13.725$, with $R^2 = 0.9805$. The LOD was determined based on the relationship with three times the standard derivation as the control signal. The LOD was as low as 245 pM. The current sensors for 17β-estradiol detection include fluorescence, enzyme sensors, electrochemical immunoassay and electrochemical sensor. Enzyme sensors obtain relatively low LOD, but they are expensive. Electrochemical sensors are simple and economical for 17β-estradiol detection. They have the advantages of fast and sensitive response. The detection sensitivity is affected by biomolecule immobilization on the electrodes. Their LOD is in the nM range. The LOD of the NIR phosphorescence aptasensor is 0.29 ng mL^{-1} and in concentrations of 0.5 ng mL^{-1} to 1.2 μg mL^{-1}. Ru complex and QD based fluorescence sensors can detect 17β-estradiol in the range of 0.08–0.4 μM with the LOD of 37 nM. Our CD and AuNP based FRET aptasensor achieves good sensitivity and a low LOD of 245 pM. It presents the advantages of low LOD, low cost and wide detection range[40–47] (Table 1).

3.6. Specificity of FRET aptasensor

To explore the specificity of the FRET aptasensor for 17β-estradiol detection, the fluorescence recovery efficiencies of detecting hydrocortisone, estriol, estrone, diethylstilbestrol and hexestrol were investigated, respectively. The fluorescence

recovery efficiencies of detecting 17β-estradiol, hydrocortisone, estriol, estrone diethylstilbestrol, and hexestrol are shown in Fig. 6. When 17β-estradiol was detected, the fluorescence intensity increased. The recovery of fluorescence intensity was obvious for 17β-estradiol, while it was not obvious for hydrocortisone, estriol and estrone detection. The fluorescence recovery efficiencies of 100 nM estradiol was 36.06%. The recovery efficiency of 100 nM hydrocortisone, estriol, estrone, diethylstilbestrol, and hexestrol were 3.95%, 8.72%, 1.35%, 2.14%, and 1.37% respectively. The recovery efficiencies of 1 nM 17β-estradiol, hydrocortisone, estriol, estrone, diethylstilbestrol, and hexestrol were 12.52%, 1.95%, 4.06%, 11.36%, 1.56% and 0.99%, respectively (Fig. S9†). Therefore, the results indicated that this FRET aptasensor showed good specificity for 17β-estradiol detection.

3.7. Sample analysis

To investigate the applicability of the FRET aptasensor, the amounts of 17β-estradiol in sea salt samples were detected. Experiments of spiked recoveries were studied by adding standard 17β-estradiol. Reasonable spiked recoveries were obtained with different concentrations of 0.4, 5, 50 and 500 nM shown in Table 2. The recoveries of sea salt samples were in the range of 88.4–114.2%, showing the potential applicability of FRET aptasensor for 17β-estradiol detection in real samples.

This FRET aptasensor is a good option for 17β-estradiol detection with easy operation, low cost, and good sensitivity. Aptamer can bind to 17β-estradiol specifically. Therefore, the FRET aptasensor presented high selectivity. The current methods for 17β-estradiol detection include HPLC, immunoassay, electrochemical detection, and so on. HPLC receives relatively precise results and is applied in the area of drug content measurement and medical diagnosis. This method requires expensive chromatographic instrumentation and complex operation procedure.[8,9] Immunoassay needs simple operation for 17β-estradiol operation, and they can be used in portable detection or rapid test strip. Immunoassay relies on a specific reaction between the antibody and antigen. Antibody can be easily affected by environmental conditions, such as pH and temperature.[39] An electrochemical aptasensor using disposable laser scribed graphene electrodes has been developed for 17β-estradiol detection with high sensitivity. It has the advantages of fast and sensitive response. However, the stability of the system is affected by conjugation of oligonucleotides on electrodes.[48,49] Our FRET aptasensor based on CDs and AuNPs

as fluorescence donor and acceptor detect 17β-estradiol in the range of 400 pM to 5.5 μM with a low LOD of 245 pM. The solubility of 17β-estradiol is 0.0015 g L^{-1}, which is relatively low at 25 °C. The recovery rate may not be increased by increasing the concentration of 17β-estradiol. Moreover, it is hard to increase the recovery rate in homogeneous FRET system. It is better to perform the detection on heterogeneous FRET system in the future work. It presents good specificity because aptamer has a specific affinity to 17β-estradiol. The "turn-on" effect can be clearly observed, and fluorescence recovery can be obtained when the target molecule is captured by aptamers. This FRET aptasensor has the potential for estrogen detection in bioanalytical and clinical diagnostic applications.

4. Conclusions

A "turn-on" FRET aptasensor based on CDs and AuNPs as fluorescence donors and receptors was developed for 17β-estradiol detection. The CD was connected with amino modified oligos (F1) *via* the EDC/NHS coupling reaction. AuNPs was connected with thiol-modified oligos (F2) by strong Au–S bond. Aptamers were complementary to Fl and F2, bringing CDs and AuNPs highly close to each other. Under UV light with the wavelength of 360 nm excitation, the FRET phenomenon occurred between CDs and AuNPs. When 17β-estradiol was detected, it was specifically bound to the aptamer. FRET phenomenon was destroyed and fluorescence was recovered. The recovery efficiency of fluorescence was calculated for a series of 17β-estradiol concentrations. The aptasensor demonstrated the feasibility of 17β-estradiol detection with the LOD of 245 pM. The experiments for hydrocortisone, estriol, estrone, diethylstilbestrol and hexestrol detection were performed as controls showing good specificity of the FRET aptasensor. Reasonable spiked recoveries were obtained in the sea salt samples. The "turn-on" FRET aptasensor has the potential to detect estrogen sensitively in food safety and environmental applications.

Conflicts of interest

The authors declare that there is no conflict of interest.

Acknowledgements

References

1 X. L. Yao, J. Gao, K. Yan, Y. X. Chen and J. D. Zhang, Ratiometric self-powered sensor for 17β-estradiol detection based on a dual-channel photocatalytic fuel cell, *Anal. Chem.*, 2020, **92**, 8026–8030.

2 Y. Wang, W. C. Zhao, R. X. Gao, S. Hussain, Y. Hao, J. H. Tian, S. H. Chen, Y. H. Feng, Y. B. Zhao and Y. Y. Qu, Preparation of lightweight daisy-like magnetic molecularly imprinted polymers via etching synergized template immobilization for enhanced rapid detection of trace 17β-estradiol, *J. Hazard. Mater.*, 2022, **424**, A127216.

3 C. Ely, I. S. Moreira, J. P. Bassin, M. W. C. Dezotti, D. P. Mesquita, J. Costa, E. C. Ferreira and P. M. L. Castro, Treatment of saline wastewater amended with endocrine disruptors by aerobic granular sludge: Assessing performance and microbial community dynamics, *J. Environ. Chem. Eng.*, 2022, **10**, 107272.

4 A. Varriale, A. Pennacchio, G. Pinto, G. Oliviero, D. S. Errico, A. Majoli and D. S. Giovanni, A fluorescence polarization assay to detect steroid hormone traces in milk, *J. Agric. Food Chem.*, 2015, **63**, 9159–9164.

5 S. Yang, D. P. Zhang, Y. X. Xu, X. B. Wang, X. Liu, S. Wang, J. Z. Wang, M. T. Wu, Z. W. He, J. Zhao and H. Yuan, Discriminating the endogenous and exogenous urinary estrogens in human by isotopic ratio mass spectrometry and its potential clinical value, *Steroids*, 2013, **78**, 297–303.

6 N. Hamid, M. Junaid and D. S. Pei, Combined toxicity of endocrine-disrupting chemicals: a review, *Ecotoxicol. Environ. Saf.*, 2021, **215**, 112136.

7 G. J. Nohynek, C. J. Borgert, D. Dietrich and K. K. Rozman, Endocrine disruption: fact or urban legend?, *Toxicol. Lett.*, 2013, **223**, 295–305.

8 C. C. Chang and S. D. Huang, Determination of the steroid hormone levels in water samples by dispersive liquid–liquid microextraction with solidification of a floating organic drop followed by high-performance liquid chromatography, *Anal. Chim. Acta*, 2010, **662**, 39–43.

9 Q. S. Zhong, Y. F. Hu, Y. L. Hu and G. K. Li, Dynamic liquid–liquid–solid microextraction based on molecularly imprinted polymer filaments on-line coupling to high performance liquid chromatography for direct analysis of estrogens in complex samples, *J. Chromatogr. A*, 2012, **1241**, 13–20.

10 P. B. Fayad, M. Prévost and S. Sauvé, On-line solid-phase extraction coupled to liquid chromatography tandem mass spectrometry optimized for the analysis of steroid hormones in urban wastewaters, *Talanta*, 2013, **115**, 349–360.

11 C. Bennetau-Pelissero, B. Arnal-Schnebelen, V. Lamothe, P. Sauvant, J. L. Sagne, M. A. Verbruggen, J. Mathey and O. Lavialle, ELISA as a new method to measure genistein and daidzein in food and human fluids, *Food Chem.*, 2003, **82**, 645–658.

12 P. Supchocksoonthorn, M. C. A. Sinoy, M. D. G. de Luna and P. Paoprasert, Facile fabrication of 17β-estradiol electrochemical sensor using polyaniline/carbon dot-coated glassy carbon electrode with synergistically enhanced electrochemical stability, *Talanta*, 2021, **235**, 122782.

13 S. Hussain, F. T. Lv, R. L. Qi, T. Senthilkumar, H. Zhao, Y. Y. Chen, L. B. Liu and S. Wang, Forster resonance energy transfer mediated rapid and synergistic discrimination of bacteria over Fungi using a cationic

conjugated glycopolymer, *ACS Appl. Bio Mater.*, 2020, **3**, 20–28.

14 C. H. M. Gary, P. Clara, A. R. Erik, T. Q. Sun and J. Zhang, A rationally enhanced red fluorescent protein expands the utility of FRET biosensors, *Nat. Commun.*, 2020, **11**, 1848.

15 X. X. Liu, Y. Y. Hou, S. R. Chen and J. W. Liu, Controlling dopamine binding by the new aptamer for a FRET-based biosensor, *Biosens. Bioelectron.*, 2021, **173**, 112798.

16 S. L. Jia, C. Q. Wang, J. Qian, X. C. Zhang, H. N. Cui, Q. Zhang, Y. M. Tian, N. Hao, J. Wei and K. Wang, An upgraded 2D nanosheet-based FRET biosensor: insights into avoiding background and eliminating effects of background fluctuations, *Chem. Commun.*, 2022, **58**, 467–470.

17 T. Watabe, K. Terai, K. Sumiyama and M. Matsuda, Booster, a red-shifted genetically encoded Forster Resonance Energy Transfer (FRET) biosensor compatible with Cyan fluorescent protein/yellow fluorescent protein-based FRET biosensors and blue light-responsive optogenetic tools, *ACS Sens.*, 2020, **5**, 719–730.

18 H. F. Sha and B. Yan, Design of a ratiometric fluorescence sensor based on metal organic frameworks and Ru(bpy) 32+-doped silica composites for 17β-Estradiol detection, *J. Colloid Interface Sci.*, 2021, **583**, 50–57.

19 Y. Y. Zhu, Y. L. Cai, L. G. Xu, L. X. Zheng, L. M. Wang, B. Qi and C. L. Xu, Building an aptamer/graphene oxide FRET biosensor for one-step detection of bisphenol A, *ACS Appl. Mater. Interfaces*, 2015, **7**, 7492–7496.

20 A. B. Iliuk, L. H. Hu and W. A. Tao, Aptamer in bioanalytical applications, *Anal. Chem.*, 2011, **83**, 4440–4452.

21 D. W. Feng, M. X. Ren, Y. F. Miao, Z. R. Liao, T. J. Zhang, S. Chen, K. D. Ye, P. J. Zhang, X. L. Ma, J. T. Ni, X. Q. Hu, H. J. Li, J. R. Peng, A. Q. Luo, L. N. Geng and Y. L. Deng, Dual selective sensor for exosomes in serum using magnetic imprinted polymer isolation sandwiched with aptamer/graphene oxide based FRET fluorescent ignition, *Biosens. Bioelectron.*, 2022, **207**, 114112.

22 Y. Zhang, J. Zhou, X. X. Zhang, W. L. Wang, C. Yang, X. L. Shi, Y. W. Feng and A. Renagul, NIR persistent luminescence nanoparticles based turn-on aptasensor for autofluorescence-free determination of 17β-estradiol in milk, *Food Chem.*, 2022, **373**, 131432.

23 X. Qi, H. Hu, Y. Yang and Y. Piao, Graphite nanoparticle as nanoquencher for 17-estradiol detection using shortened aptamer sequence, *Analyst*, 2018, **143**, 4163–4170.

24 T. Mallick, A. Karmakar, M. Kar, S. Dutta, S. K. Mondal, M. D. Mandal, A. Pramanik and N. A. Begum, Carbazole-decorated fluorescent CdS quantum dots: A potential light-harvesting material, *J. Phys. Chem. Solids*, 2022, **164**, 110603.

25 S. Y. Lu, G. J. Xiao, L. Z. Sui, T. L. Feng, X. Yong, S. J. Zhu, B. J. Li, Z. Y. Liu, B. Zou, M. X. Jin, S. T. John, H. Yan and B. Yang, Piezochromic carbon dots with two-photon fluorescence, *Angew. Chem., Int. Ed.*, 2017, **56**, 6187–6191.

26 G. Zhang, Q. H. Ji, Z. Wu, G. C. Wang, H. J. Liu, J. H. Qu and J. H. Li, Facile "spot-heating" synthesis of carbon dots/carbon nitride for solar hydrogen evolution synchronously with contaminant decomposition, *Adv. Funct. Mater.*, 2018, **28**, 1706462.

27 Q. H. Liang, W. J. Ma, Y. Shi, Z. Li and X. M. Yang, Easy synthesis of highly fluorescent carbon quantum dots from gelatin and their luminescent properties and applications, *Carbon*, 2013, **60**, 421–428.

28 W. W. Ye, M. K. Tsang, X. Liu, M. Yang and J. H. Hao, Upconversion luminescence resonance energy transfer (LRET)-based biosensor for rapid and ultrasensitive detection of avian influenza virus H7 subtype, *Small*, 2014, **10**, 2390–2397.

29 M. K. Tsang, W. W. Ye, G. J. Wang, J. M. Li, M. Yang and J. H. Hao, Ultrasensitive detection of Ebola virus oligonucleotide based on upconversion nanoprobe/nanoporous membrane system, *ACS Nano*, 2016, **10**, 598–605.

30 J. Y. Shi, C. Y. Chan, Y. K. Pang, W. W. Ye, F. Tian, J. Lyu, Y. Zhang and M. Yang, A fluorescence resonance energy transfer (FRET) biosensor based on graphene quantum dots (GQDs) and gold nanoparticles (AuNPs) for the detection of mecA gene sequence of Staphylococcus aureus, *Biosens. Bioelectron.*, 2015, **67**, 595–600.

31 A. A. Omar, K. Shalen, B. C. Zhu, T. S. Jadranka, P. M. Kenneth and M. H. Justin, Ultrasensitive colorimetric detection of 17β-estradiol: The effect of shortening DNA aptamer sequences, *Anal. Chem.*, 2015, **87**, 4201–4209.

32 A. Aghamali, M. Khosravi, H. Hamishehkar, N. Modirshahla and M. A. Behnajady, Synthesis and characterization of high efficient photoluminescent sunlight driven photocatalyst of N-carbon quantum dots, *J. Lumin.*, 2018, **201**, 265–274.

33 H. Xu, X. P. Yang, G. Li, C. Zhao and X. J. Liao, Green synthesis of fluorescent carbon dots for selective detection of Tartrazine in food samples, *J. Agric. Food Chem.*, 2015, **63**, 6707–6714.

34 S. Maiti, K. Das and P. K. Das, Label-free fluorimetric detection of histone using quaternized carbon dot–DNA nano biohybrid, *Chem. Commun.*, 2013, **49**, 8851–8853.

35 Y. Li, J. Y. Xu, M. M. Jia, Z. K. Yang, Z. W. Liang, J. J. Guo, Y. L. Luo, F. Shen and C. Y. Sun, Colorimetric determination of 17β-estradiol based on specific recognition of aptamer and the salt-induced aggregation of gold nanoparticles, *Mater. Lett.*, 2015, **159**, 221–224.

36 R. Liu, D. Wu, S. Liu, K. Koynov, W. Knoll and Q. Li, An aqueous route to multicolor photoluminescent carbon dots using silica spheres as carriers, *Angew. Chem., Int. Ed.*, 2009, **48**, 4598–4601.

37 W. J. Dong, R. P. Wang, X. J. Gong and C. Dong, An efficient turn-on fluorescence biosensor for the detection of glutathione based on FRET between N,S dual-doped carbon dots and gold nanoparticles, *Anal. Bioanal. Chem.*, 2019, **411**, 6687–6695.

38 W. Hu, T. Chen, Y. Zhang and W. W. Ye, A carbon dot and gold nanoparticle-based fluorometric immunoassay for 8-hydroxy-2′-deoxyguanosine in oxidatively damaged DNA, *Microchim. Acta*, 2019, **186**, 303.

39 Y. Zhang, H. J. Yang, Z. H. Xu, X. Liu, J. Zhou, X. F. Qu, W. L. Wang, Y. W. Feng and C. F. Peng, An ultra-sensitive

photothermal lateral flow immunoassay for 17β-estradiol in food samples, *Food Chem.*, 2023, **404**, 134482.

40 A. Q. Wang, Y. P. Ding, L. Li, D. D. Duan, Q. W. Mei, Q. Zhuang, S. Q. Cui and X. Y. He, A novel electrochemical enzyme biosensor for detection of 17β-estradiol by mediated electron-transfer system, *Talanta*, 2019, **192**, 478–485.

41 P. Xie, Z. P. Liu, S. Q. Huang, J. M. Chen, Y. Yan, N. Li, M. M. Zhang, M. L. Jin and L. L. Shui, A sensitive electrochemical sensor based on wrinkled mesoporous carbon nanomaterials for rapid and reliable assay of 17β-estradiol, *Electrochim. Acta*, 2022, **408**, 139960.

42 H. L. Huang, S. Shi, X. Gao, R. R. Gao, Y. Zhu, X. W. Wu, R. M. Zang and T. M. Yao, A universal label-free fluorescent aptasensor based on Ru complex and quantum dots for adenosine, dopamine and 17β-estradiol detection, *Biosens. Bioelectron.*, 2016, **79**, 198–204.

43 B. S. Matheus, S. S. Jaqueline, S. P. Montcharles, R. N. Letícia, P. O. Ivan, J. L. A. Alvaro, F. S. Etenaldo, G. Renato, R. F. Antonio and J. A. Gilberto, CeO₂ nanostructured electrochemical sensor for the simultaneous recognition of diethylstilbestrol and 17β-estradiol hormones, *Sci. Total Environ.*, 2022, **805**, 150348.

44 S. Preeyanuch, C. A. S. Ma, D. G. D. L. Mark and P. Peerasak, Facile fabrication of 17β-estradiol electrochemical sensor using polyaniline/carbon dot-coated glassy carbon electrode with synergistically enhanced electrochemical stability, *Talanta*, 2021, **235**, 122782.

45 Y. Zhang, J. Zhou, X. X. Zhang, W. L. Wang, C. Yang, X. L. Shi, Y. W. Feng and A. Renagul, NIR persistent luminescence nanoparticles based turn-on aptasensor for autofluorescence-free determination of 17β-estradiol in milk, *Food Chem.*, 2022, **373**, A131432.

46 P. Eloy, H. C. Fernando, P. Concepción, D. Paula, S. Alfredo, C. C. Thiago, A. S. M. Sergio, M. P. José and V. Reynaldo, Decoration of reduced graphene oxide with rhodium nanoparticles for the design of a sensitive electrochemical enzyme biosensor for 17β-estradiol, *Biosens. Bioelectron.*, 2017, **89**, 343–351.

47 W. Ademar, M. T. Anderson, L. F. Elson, F. F. Orlando and D. P. T. S. Maria, Voltammetric determination of 17β-estradiol in different matrices using a screen-printed sensor modified with CuPc, Printex 6L carbon and Nafion film, *Microchem. J.*, 2019, **147**, 365–373.

48 M. A. Nameghi, N. M. Danesh, M. Ramezani, M. Alibolandi, K. Abnous and S. M. Taghdisi, An ultrasensitive electrochemical sensor for 17β-estradiol using split aptamers, *Anal. Chim. Acta*, 2019, **1065**, 107–112.

49 Z. Chang, B. C. Zhu, J. J. Liu, X. Zhu, M. T. Xu and J. Travas-Sejdic, Electrochemical aptasensor for 17β-estradiol using disposable laser scribed graphene electrodes, *Biosens. Bioelectron.*, 2021, **185**, 113247.